

Anomalous critical slowing down of spin fluctuations in Gd observed with ¹⁶¹Dy Mössbauer effect

Ataur R. Chowdhury, Gary S. Collins, and Christoph Hohenemser

Department of Physics, Clark University, Worcester, Massachusetts 01610

(Received 13 July 1984)

Using sources of ¹⁶¹DyGd produced directly by thermal neutron irradiation of ¹⁶⁰Gd-enriched Gd metal, we have observed Mössbauer line broadening in the reduced temperature range $3 \times 10^{-4} < t < 3 \times 10^{-2}$ above T_c . The excess linewidth diverges according to the power law $\Delta\Gamma_c = Dt^{-w}$, with w in the range $0.21 < w < 0.28$ depending on fitting procedure. On the assumption that the spin fluctuations are isotropic and describable by dynamical scaling theory, we conclude that the dynamical exponent z lies in the range $1.3 < z < 1.52$. This range is anomalously low, since even with dipolar or pseudodipolar perturbations of isotropic short-range exchange interactions one expects $z=2.0$.

I. INTRODUCTION

According to general scaling theory,¹ critical dynamics for spins with short-range interactions depends on the static universality class defined by the lattice dimensionality d and order-parameter dimensionality n . Each static universality class, however, breaks up into separate dynamic subclasses, depending on what additional perturbations are present. Different dynamics are expected depending on whether perturbations are long or short range, whether they conserve order parameter or not, and whether they involve anisotropy.

Scaling theory treats the correlation length $\xi = 1/\kappa$ as the only relevant length in the problem, and defines the dynamical correlation function as

$$S_c^{zz}(\vec{q}, \omega) = \frac{2\pi S^{zz}(\vec{q}, \kappa)}{\omega_c^{zz}(\vec{q}, \kappa)} f_{q, \kappa}[\omega/\omega_c^{zz}(\vec{q}, \kappa)]. \quad (1)$$

Here, $S^{zz}(\vec{q}, \kappa)$ is the static correlation function and $\omega_c^{zz}(\vec{q}, \kappa)$ is the energy linewidth of the critical mode, given, respectively, by

$$S(\vec{q}, \kappa) = q^{-2+\eta} g(\vec{q}/\kappa), \quad (2a)$$

$$\omega_c(\vec{q}, \kappa) = q^z \Omega(\vec{q}/\kappa). \quad (2b)$$

The inverse correlation length κ carries the reduced temperature dependence, $\kappa \sim t^\nu$. The static exponents ν and η describe spatial correlations, and are linked to the susceptibility exponent γ via the static scaling relation $(2-\eta)\nu = \gamma$. The dynamical exponent z describes the time correlations. An abbreviated summary of predicted z values for several model spin systems appears in Table I. One question that can be asked about dynamics is what is the effective value of z ? Another, more detailed question is what is the form of the dynamic scaling function $\Omega(\vec{q}/\kappa)$?

TABLE I. Predictions for z . Adapted from P. C. Hohenberg and B. I. Halperin [Rev. Mod. Phys. **49**, 435 (1977)]. See also C. Hohenemser, L. Chow, and R. M. Suter [Phys. Rev. B **26**, 5056 (1982)].

Model spin system	Static universality class	Scaling law for z	Approximate value for z for $d=3$
Heisenberg ferromagnet	(3, d)	$\frac{1}{2}(d+2-\eta)$	$\frac{5}{2}$
Heisenberg antiferromagnet	(3, d)	$d/2$	$\frac{3}{2}$
Anisotropic ferromagnet	(1, d)	$2-\alpha/\nu$	2
Anisotropic antiferromagnet	(1, d)	$2-\alpha/\nu$	2
Ferromagnet with dipolar interactions	(n, d)	$2+c\eta$ $c = -0.50$	2

As shown in a recent review of spin dynamics in isotropic systems,² the first question may be answered by electron-spin resonance (ESR) which measures the relaxation rate for the uniform ($q=0$) mode, and hyperfine-interaction techniques such as Mössbauer spectroscopy, perturbed angular correlations, and nuclear magnetic resonance, which measure the spin correlation time averaged over all q . Both questions may be approached by neutron scattering—the only method which, in principle, probes spin dynamics in a differential manner.

In isotropic ferromagnets (EuS, EuO, Fe, Ni, and Co), ESR and hyperfine experiments, with the possible exception of Co, indicate that Heisenberg dynamics *fails* in the hydrodynamic limit ($q\xi \ll 1$) near T_c .^{2,3} This is demonstrated by crossover from $z=2.5$ (Heisenberg value) to $z=2.0$ (spin-nonconserved dynamics) in hyperfine experiments, and pure $z=2.0$ behavior in ESR experiments. Recently, with new high-resolution neutron experiments on Fe, it has been shown by Mezei⁴ for the first time that neutron scattering also supports the existence of non-Heisenberg spin dynamics in the hydrodynamic region, and that this is consistent with the hyperfine results.^{5,6}

The question remains as to what causes the observed crossover and the failure of Heisenberg spin dynamics in isotropic ferromagnets. Although two recent theoretical papers address the problem,^{7,8} these give only the broadest guidance on applicability to specific magnetic systems. It is therefore of interest to extend experimental work beyond the few systems that have been studied in detail to date. To this end here we report work on Gd studied via ¹⁶¹Dy Mössbauer spectroscopy. In brief, we measure the excess linewidths just above T_c , transform them via dynamic linewidth theory to spin autocorrelation times, and fit these times with a critical exponent that is directly related to the exponent z via a scaling law. Details of our analysis appear in Sec. IV. A preliminary account of the work has appeared earlier.⁹

II. THE CASE OF GADOLINIUM

Gd metal has a Curie temperature of $T_c \sim 292$ K and should exhibit little single-ion anisotropy since its magnetism is produced almost wholly by spherically symmetric $^8S_{7/2}$ Gd^{3+} ions. Because its large magnetic moment is localized in the small $4f$ shell, Gd should, in principle, be better approximated by the Heisenberg model than the partially itinerant magnets Fe and Ni. A review of the literature suggests, however, that this view may be too simple.

A. Magnetic structure

The crystalline structure of Gd is hexagonal close packed with a nearly ideal c/a ratio of 1.59. This suggests that Gd will have little magnetocrystalline anisotropy. Well above T_c , isotropic spin interactions are supported by the equality of paramagnetic Curie temperatures measured parallel and perpendicular to the c axis.¹⁰ Below T_c the easy direction of magnetization is strongly temperature dependent. Up to $T_0 \sim 230$ K, neutron diffraction¹¹ and crystalline anisotropy^{12,13} shows that the angle between the c axis and the easy axis is about

30° – 60° . For $T_0 < T < T_c$ the average spin alignment is along the c axis. Single-crystal ¹⁵⁵Gd Mössbauer studies¹⁴ indicate that the anisotropy at 4.2 K depends on the crystalline form and impurity content, which leads the authors to speculate that Gd^{3+} may not be a pure $S_{7/2}$ ion.

B. Static critical exponents

Many “isotropic” magnetic systems are anisotropic below T_c . Fe and Ni have well-defined easy-magnetization directions along $\langle 100 \rangle$ and $\langle 111 \rangle$, respectively, and in MnF_2 the average spin alignment is along the c axis. If anisotropy persists near T_c , as in the case of MnF_2 , the magnetic system exhibits static critical behavior characteristic of the $(d,n)=(3,1)$ Ising model; if, on the other hand, the anisotropy vanishes near T_c , as in the case of Fe and Ni, the magnetic system shows static critical behavior characteristic of the $(d,n)=(3,3)$ Heisenberg model.¹⁵

To determine what happens in Gd in the critical region, we have reviewed available measurements of static critical exponents. In compiling the results we were guided by the empirical finding¹⁶ that valid asymptotic behavior in $d=3$ systems is assured only if the range of reduced temperature is restricted to $t < 10^{-2}$. By this criterion, some published results are almost certainly nonasymptotic, and hence uninteresting. The remainder of the measurements^{17–26} are summarized in Table II and should be compared to the best theoretical predictions,²⁷ given in Table III. As can be seen from the temperature ranges quoted in Table II, even these selected measurements contain some data from the nonasymptotic region, and one should therefore not expect close agreement with the theory.

Arguing for isotropic (Heisenberg) behavior are negative values of α and values of β that are, with one exception, near the Heisenberg-model prediction. Arguing for anisotropic (Ising) behavior are low values of γ that lie close to predictions for the Ising model. Also indicative of possible Ising behavior is the observation¹⁹ that the domain walls appear to transform from Bloch (Heisenberg) character far from T_c to Ising character close to T_c .

When the results of different experiments are combined, the static scaling law $\alpha + 2\beta + \gamma = 2$ is rather badly violated. This suggests that one or more of the quoted exponents is a nonasymptotic “effective” value that is subject to corrections-to-scaling modification. Such errors are particularly important for γ , where a 5–10% scaling correction can have a major effect. In the case of the two experiments fitted with scaling equations of state, the deduced values of δ are far different than either the Ising- or Heisenberg-model predictions. This suggests that the data are systematically affected either by an insufficiently close approach to T_c , or applied fields that are too large for the observation of asymptotic critical behavior.

We conclude from our review of static critical behavior that Gd is probably isotropic. Perhaps the strongest argument against Ising character is the negative sign of α , which would have to change to support Ising critical behavior. However, our conclusion is not unqualified, because large ($\sim 10\%$) scaling corrections disturb the quoted

TABLE II. Selected static critical exponent measurements for Gd.

Exponent	Range of t	Value	Reference	Comment
α	$10^{-3}-10^{-1}$	-0.09(5)	17	Significant rounding may account for $\alpha \neq \alpha'$.
α'	$10^{-3}-10^{-1}$	-0.32(5)		
α		-0.20(2)	18	Fitted with scaling equation which assumes $\alpha = \alpha'$.
α'		-0.20(2)		
β	$1.7 \times 10^{-3}-6 \times 10^{-1}$	0.385	19	Derived from Barkhausen noise power. Experiment shows crossover to Ising like domain walls near T_c .
β	$3 \times 10^{-3}-5 \times 10^{-2}$	0.31(5)	20	Derived from ferromagnetic transmission resonance in zero field.
β	$2.7 \times 10^{-2}-0.19$ $< 2.7 \times 10^{-2}$	0.39 > 0.39	21	Rounding may account for increase in β for small t .
γ	$2 \times 10^{-3}-2 \times 10^{-1}$	1.3(1)	22	Reanalysis of Graham's data (Ref. 23)
γ		1.24(3)	24	
β	$ t > 2 \times 10^{-3}$	0.37(1)	25	Scaling-equation analysis of Graham's data, which assumes $\gamma = \beta(\delta - 1)$.
γ		1.25		
δ		4.39(10)		
β	$ t > 4 \times 10^{-3}$	0.381(15)	26	Scaling-equation analysis which assumes $\gamma = \beta(\delta - 1)$.
γ		1.196		
δ		3.615(15)		

experimental results and prevent quantitative agreement with scaling laws.

C. Dynamic behavior near T_c

Quasielastic neutron scattering on a ^{160}Gd -enriched single crystal²⁸ indicates the presence of anisotropic short-range order above and below T_c , but does not probe inelastic, small- q diffusive scattering in the critical region. To date, only the ESR work of Burgardt and Seehra²⁹ probes the spin dynamics of Gd near T_c . Working at 9 GHz, with applied fields of 0.1–0.3 T, these workers observed *broadening* of the ESR line as $T \rightarrow T_c^+$. This may be interpreted as “critical speeding up” predicted for the

TABLE III. Theoretical static critical exponents for $d=3$ magnetic systems. Values of β and γ are from J. C. Le Guillou and J. Zinn-Justin [Phys. Rev. Lett. **39**, 95 (1977)]. Values of α and δ are calculated from β and γ via the scaling relations $\alpha + 2\beta + \gamma = 2$ and $\gamma = \beta(\delta - 1)$.

Exponent	Ising model	Heisenberg model
α	0.110(2)	-0.116(2)
β	0.325(1)	0.365(1)
γ	1.240(1)	1.387(1)
δ	4.816(3)	4.797(3)

exchange-dominated critical region $4\pi\chi < 1$.^{30–33} In contrast to experimental work by Kötzer and von Philipsborn³⁴ on CdCr_2Se_4 , the power law for the $q=0$ Onsager coefficient in Gd is much weaker than predicted, i.e., $\Gamma \sim \chi^{0.84}$ compared to $\Gamma \sim \chi^{7/4}$. This probably results from the large applied fields used. Kötzer and Philipsborn found, for CdCr_2Se_4 , that the predicted $7/4$ power law occurs only for small fields (low frequency), and that high fields suppress the divergence of Γ .

In whatever way the ESR data on Gd is construed, they cannot be interpreted as asymptotic behavior involving critical slowing down and a *narrowing* of the ESR linewidth as $T \rightarrow T_c^+$. In this sense the existing data are irrelevant to the asymptotic critical region. Other work on the ESR linewidth, for example, on EuO ,^{35,36} makes clear that to observe critical slowing down it is necessary to use zero or small applied fields.

III. EXPERIMENT

The choice of the ^{161}Dy Mössbauer probe is based primarily on the very large hyperfine coupling [$A_e = \gamma_e H_{\text{hf}}(0)/S = 1.925 \times 10^9 \text{ s}^{-1}$; $A_g = \gamma_g H_{\text{hf}}(0)/S = -1.540 \times 10^9 \text{ s}^{-1}$], which is comparable to the sensitive ^{100}Rh perturbed-angular-correlation probe.² The large hyperfine coupling, in turn, enables Mössbauer measurements over a wide range of reduced temperature, in con-

trast to studies using the insensitive ^{57}Fe probe.³⁷ Previous work on Gd^{161}Dy shows that the favorable features of the probe can, in fact, be realized, although there is no clear-cut evidence in the literature on critical line broadening near T_c .³⁸

Sources of ^{161}Tb in Gd were made by thermal neutron irradiation of a 98.7 at. % ^{160}Gd -enriched, 99.99%-pure Gd-metal foils obtained from Oak Ridge National Laboratory. The total neutron dose, provided by the Massachusetts Institute of Technology Research Reactor, was approximately 10^{18} n/cm², and produced a source activity of about 5 mCi. The absorber consisted of 91 at. % enriched ^{161}Dy in the form of DyF_3 , prepared as described by Wit.³⁹

Because the ^{161}Dy Mössbauer line is relatively insensitive to radiation-damage effects, we studied the problem with ^{111}In perturbed γ - γ angular correlation (PAC).⁴⁰ For this purpose, we diffused 2.7-d ^{111}In into a small piece of the enriched Gd foil by depositing the activity on the surface and heating *in vacuo* for 45 min at 850°C. The PAC signal consisted of a single, undamped quadrupole precession, with coupling frequency

$$\omega_0 = (3\pi/10)e^2Qq_{zz} = 23.4(7) \text{ Mrad/s}$$

(Fig. 1, top), which we interpreted as substitutional ^{111}In , previously seen by Boström *et al.*⁴¹ Next, we subjected the sample to the same neutron dose as the enriched Mössbauer source, with the result that the PAC spectrum became strongly damped (Fig. 1, bottom). Upon annealing at 850°C for 12 h, the damping disappeared and the

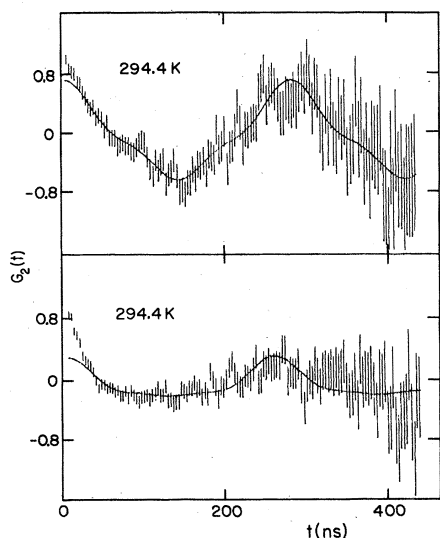


FIG. 1. Perturbed-angular-correlation spectra of a ^{160}Gd sample measured above T_c . Immediately after diffusion of ^{111}In , the observed quadrupole precessional signal (top) exhibits nearly full anisotropy, indicating that most In atoms are on defect-free, substitutional sites. After subsequent neutron irradiation, the PAC signal (bottom) is strongly damped, indicating lattice damage near the In probes. After an additional annealing treatment, the spectrum (not shown) recovered to a large, undamped anisotropy, as in the top figure.

signal returned to the form seen prior to irradiation. Guided by the extensive literature on lattice defects observed via ^{111}In PAC,⁴⁰ we conclude that the neutron irradiation produces frozen-in lattice defects in the neighborhood of the ^{111}In . These migrate to sinks when the sample is heated, leaving the sample essentially free of radiation damage.

In earlier work⁹ we used the source foil as it came out of the reactor. In contrast, all data reported here were obtained with Mössbauer sources that had been annealed in the same way as the ^{111}In -doped samples. This annealing produced a small reduction in the linewidth far above T_c , from 8.1(1) to 7.2(1) mm/s, and a significant reduction in the linewidth close to T_c .

For critical-phenomena experiments, the source temperature was varied using a two-stage thermoelectric module mounted in a vacuum can. The temperature was regulated via a feedback system employing a differential voltmeter, as in previous work.² Temperature stability over the experimental range of 273–423 K was better than 0.05 K.

Mössbauer spectra were obtained with a high-speed

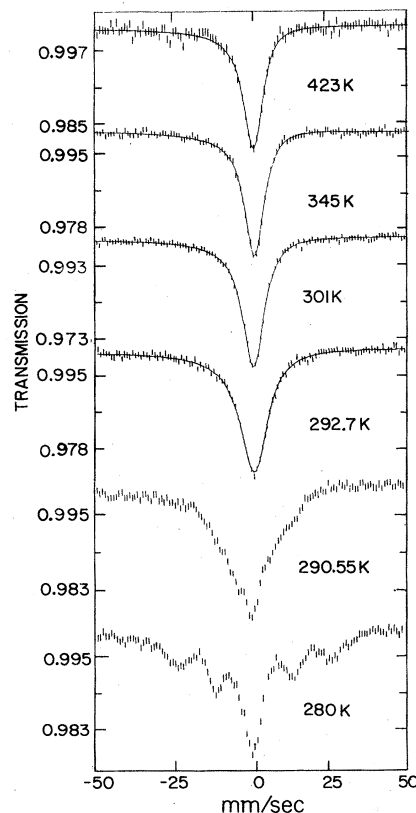


FIG. 2. Mössbauer spectra of ^{161}Dy in Gd. Far above $T_c=292.60$ K, the spectra consist of a single temperature-independent Lorentzian line (423 and 345 K). As $T \rightarrow T_c^+$, the spectra remain Lorentzian in shape but broaden due to critical slowing down of the electronic spins (301 and 292.7 K). Below T_c the spectra are non-Lorentzian due to magnetic hyperfine splitting which is unresolved close to T_c , at 290.55 K, and partly resolved at 280 K.

(± 60 cm/s) drive (Elscont model MDF-N-5) used in the constant-acceleration mode and calibrated via laser interferometry.

With the source clamped into the oven and the absorber mounted externally on a vertically driven rod, Mössbauer spectra were obtained in a temperature range $273 < T < 423$ K. Well below T_c , in a region $273 < T < 290$ K, resolved hyperfine structure was observed as previously reported by Lukashevich *et al.*³⁸ Well above T_c , in a region $345 < T < 423$ K, a single Lorentzian having a constant width of 7.2 mm/s was seen. Although this is 22 times the natural linewidth for ^{161}Dy , it is narrower than the value ~ 10 mm/s observed in the earlier work.³⁸

In the range $T - T_c < 10$ K (see Fig. 2), the linewidth diverges with decreasing temperature, as expected for the critical slowing of spin fluctuations. As in previous studies on Ni and Fe employing the ^{57}Fe Mössbauer effect,³⁷ the linewidth continues to increase as the sample enters the region of ferromagnetic ordering because initially the magnetic hyperfine structure is unresolved. This makes direct determination of T_c from the linewidth data difficult. An estimate of T_c is possible, however, by noting the region in which the line shape becomes distinctly non-Lorentzian, which occurs at the onset of static magnetic splitting. For the data reported here, a transition to non-Lorentzian line shape occurred in the range $290.5 < T < 292.5$ K, in good agreement with published estimates of T_c for Gd.

To determine T_c more precisely we again resorted to an

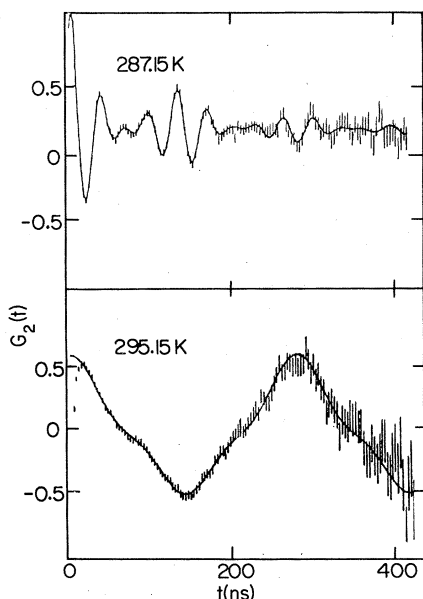


FIG. 3. Perturbed-angular-correlation spectra of an ^{111}In -doped Gd foil. Comparison of the spectra illustrates the dramatic difference between perturbation functions of spectra measured above and below T_c . For $T < T_c$ (top), spectra exhibit complex and small root-mean-square amplitude signals caused by combined magnetic and quadrupole hyperfine interactions; for $T > T_c$ (bottom), spectra involve large rms signals due solely to quadrupole interaction.

^{111}In PAC experiment. We took a small piece of the enriched sample, doped it with ^{111}In as described earlier, and irradiated and annealed it in a manner identical to the treatment of the Mössbauer source. The resulting PAC source shows a well-defined quadrupole precession above T_c as before, and exhibits a combined magnetic-quadrupole signal below T_c (see Fig. 3). To determine T_c we force-fit all the spectra with the pure quadrupole signal. As a result, the effective site fraction plotted against T develops a sharp break, due to misfitting, which we interpret as the onset of ferromagnetism (see Fig. 4). By performing measurements using the same thermoelectric heater and thermocouples as in the Mössbauer spectroscopy, we obtain $T_c = 292.60(5)$ K. As in most other critical phenomena studies, the quoted accuracy of this result is relative to other temperatures measured in our experiment, and should not be construed as accuracy on the absolute Kelvin scale.

IV. RESULTS AND INTERPRETATION

Measured linewidths and reduced temperatures are given in Table IV. All line shapes above T_c could be well fitted with a single Lorentzian. To interpret the results we separate noncritical from critical line broadening, and calculate spin autocorrelation times from the latter, according to the following four-step argument.

(1) The experimental linewidth far above T_c is written as

$$\Gamma_{\text{expt}} = \Gamma_0 + \Delta\Gamma_{\text{nc}}, \quad (3)$$

where Γ_0 is the natural linewidth and $\Delta\Gamma_{\text{nc}}$ describes non-critical broadening in both source and absorber, believed to be predominantly due to paramagnetic spin fluctuations. $\Gamma_0 + \Delta\Gamma_{\text{nc}}$ is found from the average values of Γ_{expt} far above T_c and appears to have no discernible temperature dependence.

(2) As $T \rightarrow T_c^+$ we write the experimental linewidth as

$$\Gamma_{\text{expt}} = \Gamma_0 + \Delta\Gamma_{\text{nc}} + \Delta\Gamma_c, \quad (4)$$

where $\Delta\Gamma_c$ is produced by critical spin fluctuations. Thus we assume that noncritical and critical spin fluctuations produce additive terms in the experimental linewidth.

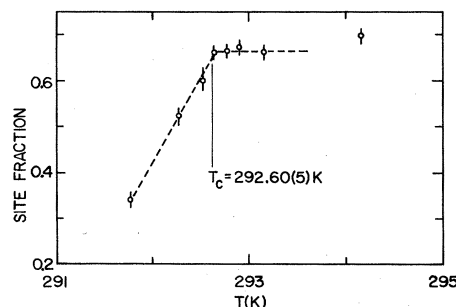


FIG. 4. Root-mean-square signal amplitudes of PAC spectra of the ^{111}In -doped, neutron-irradiated, and annealed Gd foil. The sharp break in the amplitudes was used to provide the estimate $T_c = 292.60(5)$ K, independent of the ^{161}Dy Mössbauer measurements.

TABLE IV. Γ_{expt} , $\Delta\Gamma_c$, and τ_c values for $^{161}\text{DyGd}$.

T (K)	$t=(T-T_c)/T_c^a$ (10^{-4})	Γ_{expt} (mm/s)	$\Delta\Gamma_c = \Gamma_{\text{expt}} - \Delta\Gamma_{\text{nc}} - \Gamma_0$ (mm/s)	τ_c (10^{-13} s)
292.70	3.4	10.41(14)	3.20(16)	3.99(21)
292.80	6.8	9.84(13)	2.63(16)	3.28(20)
292.93	11.1	9.90(16)	2.69(18)	3.35(23)
293.03	14.5	9.54(13)	2.33(16)	2.90(20)
293.13	17.9	9.34(14)	2.13(14)	2.65(18)
293.28	23.1	9.35(11)	2.14(14)	2.67(18)
293.48	29.9	9.25(13)	2.04(16)	2.54(20)
293.75	39.3	9.03(13)	1.82(16)	2.27(20)
294.25	56.4	8.96(13)	1.75(16)	2.18(20)
294.65	70.0	8.67(11)	1.46(14)	1.82(18)
295.15	87.1	8.52(11)	1.31(14)	1.63(18)
295.65	104	8.39(11)	1.18(14)	1.47(18)
296.50	133	8.33(11)	1.12(14)	1.39(18)
297.65	173	8.40(11)	1.19(14)	1.48(18)
299.15	224	8.13(10)	0.92(13)	1.14(17)
301.25	294	8.09(9)	0.88(13)	1.09(16)
305.20	431	7.81(11)	0.60(14)	0.75(18)
307.20	499	7.65(12)	0.44(15)	0.55(18)
310.08	597	7.45(9)	0.24(13)	0.30(16)
315.10	769	7.40(9)	0.19(13)	0.23(16)
325.15	1110	7.54(13)	0.33(16)	0.41(20)
345.0	1790	7.22(11)	(0)	(0)
373.0	2750	7.22(15)	(0)	(0)
423.0	4460	7.20(19)	(0)	(0)

^aObtained using $T_c=292.60(5)$ K. All data have a uniform error of 1.7×10^{-4} due to the uncertainty in T_c .

(3) Under the assumption that the spin fluctuations are isotropic, we interpret $\Delta\Gamma_c$ in terms of the linewidth theory of Bradford and Marshall,⁴² as extended by Hartmann-Boutron,⁴³ according to which the nuclear relaxation rate is

$$\tau_R^{-1} = C_{\text{hf}}^{\text{ME}} \tau_c = (1.04 \times 10^{21} \text{ s}^{-2}) \tau_c, \quad (5)$$

where τ_c is the spin autocorrelation time and $C_{\text{hf}}^{\text{ME}}$ is the dynamic coupling parameter appropriate for the Mössbauer effect transition.⁴⁴ In terms of τ_R^{-1} , the Mössbauer line broadening is $\Delta\Gamma_c = (\hbar c/E_\gamma) \tau_R^{-1} = (8.01 \times 10^{12} \text{ mm/s}^2) \tau_c$.⁴⁴ The results of this analysis lead to the values of $\Delta\Gamma_c$ and τ_c tabulated in Table IV.

(4) By definition, the spin autocorrelation time is

$$\tau_c = \int S_c^{\text{zz}}(\vec{q}, 0) \vec{d}q, \quad (6)$$

which, for the dynamic scaling form of $S_c^{\text{zz}}(\vec{q}, \omega)$, leads to a reduced temperature dependence,²

$$\tau_c = Dt^{-w}, \quad w = \nu(z + 2 - d - \eta) \quad (7)$$

where d is lattice dimensionality, z and η are defined by Eqs. (2a) and (2b), and ν describes the divergence of the correlation length.

For the reduced temperature range $3 \times 10^{-4} < t < 3 \times 10^{-2}$, a least-squares fit to Eq. (7) with T_c fixed at 292.60 K leads to (see Fig. 5)

$$w = 0.28(2), \quad D = 0.36(3) \text{ mm/s} = 4.5 \times 10^{-14} \text{ s}.$$

If the maximum included value of t is successively reduced, the fitted exponent and amplitude approach the ‘‘asymptotic’’ values

$$w = 0.21(3), \quad D = 0.57(6) \text{ mm/s} = 7.0(7) \times 10^{-14} \text{ s}.$$

With the theoretical Heisenberg values²⁷ of $\nu=0.705(1)$ and $\eta=0.034$, this leads to $z=1.33(3)$ and $1.43(3)$, depending on whether the ‘‘asymptotic’’ or full range of t is used, respectively. If the measured susceptibility exponent for Gd is used to estimate $\nu=\gamma/2=0.62(2)$, the corresponding results for z are 1.37(4) and 1.48(4). Taking into

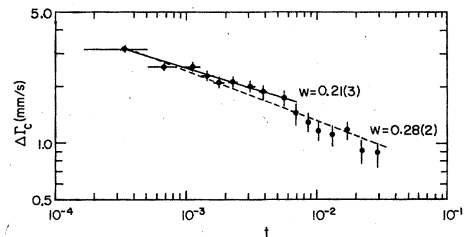


FIG. 5. Critical line broadening $\Delta\Gamma_c$ above $T_c=292.60$ K as a function of reduced temperature t . The dashed curve indicates the best fit of $\Delta\Gamma_c$ to a power-law dependence t^{-w} over the range $3 \times 10^{-4} < t < 3 \times 10^{-2}$. The solid curve indicates the fitted result over a more asymptotic range, $3 \times 10^{-4} < t < 5 \times 10^{-3}$. Neither value of w can be explained by theoretical predictions. Owing to uncertainty in background line broadening, data points for $t > 3 \times 10^{-2}$ are not plotted here.

account all assumptions and approaches to fitting our estimate of z falls into the range $1.30 < z < 1.52$. This is far below any of the predictions for ferromagnets summarized in Table I.

V. DISCUSSION

Each of the four steps leading to our interpretation of the data requires some explanation and qualification, as follows.

A. Noncritical line broadening

We attribute $\Delta\Gamma_{nc}$ to paramagnetic spin fluctuations for three reasons. (1) The static electric field gradient arising from the noncubic Gd lattice leads to an estimated quadrupole splitting of ± 1 mm/s,⁴⁵ which is too small to explain the linewidth. (2) The electric field gradient of the $4f$ ion leads to estimated splittings of ± 20 mm/s at low temperature, but decreases more rapidly than the hyperfine field as $T \rightarrow T_c^-$, and should therefore be negligible above T_c .⁴⁶ (3) Because we know of no other sources of broadening, this leaves only noncritical spin fluctuations as the source of $\Delta\Gamma_{nc}$. Because the contributions from source and absorber are not separable, an upper limit on the spin correlation time in the source is derived by attributing all of $\Delta\Gamma_{nc}$ to the ¹⁶¹DyGd source. This leads to a spin correlation time $\tau_{nc} < 9 \times 10^{-13}$ s.

B. Additivity of line broadening

The additivity of line broadening expressed in Eq. (4) is equivalent to assuming the additivity of the corresponding nuclear relaxation rates τ_R^{-1} ; this follows from the assumption that the total correlation function is additively separable into terms describing critical and noncritical fluctuations:

$$S^{zz}(\vec{q}, \omega) = S_c^{zz}(\vec{q}, \omega) + S_{nc}^{zz}(\vec{q}, \omega). \quad (8)$$

This assumption seems reasonable because the q dependence of each term is quite different. $S_c(\vec{q}, \omega)$ is dominated by long-range (small- q) fluctuations,¹ whereas $S_{nc}(\vec{q}, \omega)$ is weighted strongly by short-range (large- q) fluctuations.

C. Line-broadening theory

The use of the Bradford-Marshall and/or Hartmann-Boutron expressions for the line broadening assumes an isotropic hyperfine interaction of the form

$$\mathcal{H} = A \vec{I} \cdot \vec{S} \quad (9)$$

between the nuclear and electronic spin I and S . It also assumes that the inequality

$$\tau_c \omega_L(0) \ll 1 \quad (10)$$

is satisfied, where the nuclear Larmor frequency,

$$\omega_L(0) = \mu_I H_{hf}(0) / I \hbar S,$$

μ_I is the nuclear moment, and $H_{hf}(0)$ is the zero-temperature hyperfine field. Given Eq. (9), the inequality

(10) is certainly satisfied: For the longest value of τ_c , $\tau_c \omega_L(0) \sim 6 \times 10^{-3}$.

For an anisotropic hyperfine interaction,⁴²

$$\mathcal{H} = A I_z S_z + B (I_x S_x + I_y S_y), \quad (11)$$

the analog of Eq. (5) involves longitudinal and transverse correlation times, τ_c^{\parallel} and τ_c^{\perp} . If these have different temperature dependences (e.g., only τ_c^{\parallel} becomes singular near T_c), the resulting Mössbauer spectrum consists of a sum of Lorentzians with different temperature dependences for the line broadening. Such a spectrum would develop a distinctly non-Lorentzian line shape above T_c with an "effective" broadening that may not accurately follow the temperature dependence of the critical correlation time. The fact that we do not detect non-Lorentzian broadening suggests that the spin fluctuations are isotropic; but this conclusion is valid only within the limits of the statistical quality of our spectra, illustrated in Fig. 2.

D. Dynamic scaling theory

By definition, the experimentally measured correlation time is an integral property of the correlation function, as indicated in Eq. (6). The particular scaling law (7) is, however, the specific consequence of the assumed form of the correlation function in the critical region, given by Eqs. (1) and (2). The deduced value of z therefore depends on this assumption. Should the correlation function deviate from the assumed scaling form, any conclusions about z become meaningless. With the correlation function as stated in Eqs. (1) and (2), the integral of Eq. (6) is weighted toward $\kappa/q \sim 1$.⁴⁷ This is a constraint on the Mössbauer results that must be remembered if they are compared in the future to other measurements of critical fluctuations, such as ESR or neutron scattering.

VI. SUMMARY AND CONCLUSION

We have observed critical slowing of spin fluctuations in Gd via line broadening of ¹⁶¹DyGd Mössbauer spectra above T_c . Our interpretation of the observed line broadening indicates that the divergence of the q -averaged spin correlation time is weaker than expected for several dynamic universality classes (summarized in Table III). On the assumption that the dynamical scaling form of the correlation function is correct, our estimate for the value of the dynamical exponent z lies in the range $1.30 < z < 1.52$.

Although we do not believe it to be the case, it is possible that the anomalous value of z originates in incorrect assumptions made in interpreting the Mössbauer line broadening. The most serious potential source of concern is that spin fluctuations may become anisotropic as $T \rightarrow T_c^+$, with different temperature dependences for the longitudinal and transverse correlation times. ESR and/or neutron-scattering measurements on single crystals can, in principle, resolve this issue, and are strongly recommended.

ACKNOWLEDGMENTS

This research was supported in part by National Science Foundation Grants No. DMR-80-02443 and No. DMR-83-03611. The ^{160}Gd neutron irradiations were

performed at the MIT Research Reactor with the help of Lincoln Clark and William Fecych, and with support of a Department of Energy reactor-sharing grant. The perturbed-angular-correlation experiments were done with the helpful assistance of Carl Allard.

- ¹P. C. Hohenberg and B. I. Halperin, *Rev. Mod. Phys.* **49**, 435 (1977).
- ²C. Hohenemser, L. Chow, and R. M. Suter, *Phys. Rev. B* **26**, 5056 (1982).
- ³M. B. Salamon, *Phys. Rev.* **155**, 224 (1967).
- ⁴F. Mezei, *Phys. Rev. Lett.* **49**, 1096 (1982).
- ⁵C. Hohenemser, G. S. Collins, R. M. Suter, and L. Chow, *Phys. Rev. Lett.* **50**, 1877 (1983).
- ⁶F. Mezei, *Phys. Rev. Lett.* **50**, 1878 (1983).
- ⁷D. L. Huber, *Solid State Commun.* **48**, 831 (1983).
- ⁸J. Kötzler, *Phys. Rev. Lett.* **51**, 833 (1983).
- ⁹A. R. Chowdhury, G. S. Collins, and C. Hohenemser, *Hyperfine Interact.* **15-16**, 617 (1983).
- ¹⁰S. Legvold, in *Ferromagnetic Materials*, edited by E. P. Wohlfarth (North-Holland, Amsterdam, 1980), Vol. 1, p. 183.
- ¹¹G. Will, R. Nathans, and A. J. Alperin, *J. Appl. Phys.* **35**, 1045 (1964); J. W. Cable and E. O. Wollan, *Phys. Rev.* **165**, 733 (1968).
- ¹²W. D. Corner, W. C. Roe, and K. N. R. Taylor, *Proc. Phys. Soc. London* **80**, 927 (1962).
- ¹³F. Milstein and L. B. Robinson, *Phys. Rev.* **177**, 904 (1969).
- ¹⁴E. R. Bauminger, A. Diamant, I. Felner, I. Nowik, and S. Ofer, *Phys. Rev. Lett.* **15**, 962 (1975).
- ¹⁵K. Stierstadt, R. Anders, and W. von Hörsten, *Experimental Values of Critical Exponents and Amplitude Ratios at Magnetic Phase Transitions*, No. 20-1 of *Physics Data* (Fach-Informationen zentrum, Karlsruhe, Federal Republic of Germany, 1984). This provides extensive documentation of experimental values of critical exponents on which the conclusions in the text may be based.
- ¹⁶R. M. Suter and C. Hohenemser, *J. Appl. Phys.* **50**, 1814 (1979).
- ¹⁷E. A. S. Lewis, *Phys. Rev. B* **1**, 4368 (1970).
- ¹⁸D. S. Simons and M. B. Salamon, *Phys. Rev. B* **10**, 4680 (1974).
- ¹⁹P. Molho and J. L. Porteseil, *J. Phys. (Paris)* **44**, 83 (1983).
- ²⁰P. Sheng, C. N. Manikopoulos, and T. R. Carver, *Phys. Rev. Lett.* **30**, 234 (1973). See also C. N. Manikopoulos, P. Sheng, and T. R. Carver, *Phys. Rev. B* **8**, 1131 (1973).
- ²¹A. G. A. M. Saleh and N. H. Saunders, *J. Magn. Magn. Mater.* **29**, 197 (1982).
- ²²P. Heller, *Rep. Prog. Phys.* **30**, 731 (1967).
- ²³C. D. Graham, Jr., *J. Appl. Phys.* **36**, 1135 (1965).
- ²⁴G. H. J. Wantenaar, S. J. Campbell, D. Chaplin, T. J. McKenna, and G. V. H. Wilson, *J. Phys. C* **13**, L863 (1980).
- ²⁵M. Vicentini-Missoni, R. I. Joseph, M. S. Green, and J. M. H. L. Sengers, *Phys. Rev. B* **1**, 2312 (1970).
- ²⁶M. N. Deschizeaux and G. Develey, *J. Phys. (Paris)* **32**, 319 (1971).
- ²⁷J. C. Le Guillou and J. Zinn-Justin, *Phys. Rev. Lett.* **39**, 95 (1977).
- ²⁸H. R. Child, *Phys. Rev. B* **18**, 1247 (1978); J. W. Cable, N. Wakabayashi, and R. M. Nicklow, *J. Appl. Phys.* **52**, 2231 (1981).
- ²⁹P. Burgardt and M. S. Seehra, *Phys. Rev. B* **16**, 1802 (1977).
- ³⁰E. Riedel and F. Wegner, *Phys. Rev. Lett.* **24**, 730 (1970).
- ³¹M. S. Seehra and D. L. Huber, in *Magnetism and Magnetic Materials—1974 (San Francisco)*, *Proceedings of the 20th Annual Conference on Magnetism and Magnetic Materials*, edited by C. D. Graham, G. H. Lander, and J. J. Rhyne (AIP, New York, 1975), p. 261.
- ³²R. Raghavan and D. L. Huber, *Phys. Rev. B* **14**, 1185 (1976).
- ³³W. Finger, *Phys. Lett.* **26A**, 543 (1968).
- ³⁴J. Kötzler and H. von Philipsborn, *Phys. Rev. Lett.* **40**, 790 (1978).
- ³⁵J. Kötzler, W. Scheithe, R. Blickhan, and E. Kaldis, *Solid State Commun.* **26**, 641 (1978).
- ³⁶R. A. Dunlap and A. M. Gottlieb, *Phys. Rev. B* **22**, 3422 (1980).
- ³⁷M. A. Kobeissi, R. Suter, A. M. Gottlieb, and C. Hohenemser, *Phys. Rev. B* **11**, 2455 (1975). See also M. A. Kobeissi, *Phys. Rev. B* **24**, 2380 (1980).
- ³⁸I. I. Lukashovich, V. V. Sklyarevskii, K. P. Aleshin, B. N. Samoilov, E. P. Stepanov, and N. I. Filippov, *Zh. Eksp. Teor. Fiz. Pis'ma Red* **3**, 81 (1966) [*JETP Lett.* **3**, 50 (1966)].
- ³⁹H. P. Wit, Ph.D. thesis, University of Groningen, 1976.
- ⁴⁰F. Pleiter and C. Hohenemser, *Phys. Rev. B* **25**, 106 (1982).
- ⁴¹Boström, G. Liljegen, B. Jonsson and E. Karlsson, *Phys. Scr.* **3**, 175 (1971).
- ⁴²E. Bradford and W. Marshall, *Proc. Phys. Soc. London* **87**, 731 (1966).
- ⁴³F. Hartmann-Boutron, *Rev. Appl. Phys. (Paris)* **18**, 431 (1983).
- ⁴⁴With a saturation hyperfine field of $H_{\text{hf}}(0) = 596$ T, electronic spin $S = \frac{7}{2}$, excited- and ground-state nuclear spins and moments $I_e = I_g = +\frac{5}{2}$, $\mu_e = 0.59$ nm, and $\mu_g = -0.472$ nm, we obtain $A_e = \gamma_e H_{\text{hf}}(0)/S = 1.925 \times 10^9 \text{ s}^{-1}$ and $A_g = \gamma_g H_{\text{hf}}(0)/S = -1.540 \times 10^9 \text{ s}^{-1}$. To calculate the hyperfine coupling constant defined in Eq. (5) we use Eq. (46) of Hartmann-Boutron (Ref. 43) to obtain $C_{\text{hf}}^{\text{ME}} = 1.04 \times 10^{21} \text{ s}^{-2} = 8.01 \times 10^{12} \text{ mm}^2/\text{s}^2$. (The general equation for $C_{\text{hf}}^{\text{ME}}$ given by Hohenemser *et al.* [Ref. 2, Eq. (15b)], has an algebraic error.)
- ⁴⁵The point-charge lattice sum electric field gradient (EFG) [J. B. Fechner, M. Forker, and G. Schäfer, *Z. Phys.* **265**, 197 (1973)] was assumed to be enhanced by the antishielding factor $1 - \gamma_\infty \sim 75$ and by a factor of ~ 2 to account for conduction-electron screening [K. Shimizu, H. Mizutani, and J. Itoh, *J. Phys. Soc. Jpn.* **43**, 57 (1977)], yielding $2.6 \times 10^{17} \text{ V cm}^{-2}$. For the nuclear quadrupole moments of the $I = \frac{5}{2}$ excited and ground states of ^{161}Dy , $Q_e = Q_g = 1.36$, the corresponding seven-line Mössbauer spectrum will have maximum splittings of ± 1.2 mm/s to either side of the centroid.
- ⁴⁶The EFG caused by the (nonspherical) $4f$ -electron shell is $59 \times 10^{17} \text{ V cm}^{-2}$ at $T = 0$ K, but decreases rapidly with temperature as more crystal-field levels of the $J = \frac{15}{2}$ Dy ion become populated. [E. Karlsson, M. M. Bajaj, and L. Boström, *Phys. Scr.* **2**, 60 (1970).]
- ⁴⁷B. I. Halperin and P. C. Hohenberg, *Phys. Rev.* **177**, 952 (1968).